INFLUENCE OF MASONRY ON INFILLED FRAME WITH AND WITHOUT OPENING

Thi Thu Nga Nguyen[1,*], Nam Hung Tran[1]

[1]*Le Quy Don Technical University*

Abstract

The effect of masonry infills on the global response of frames is widely recognized but it is often neglected in the analytical models. Because of lack of effectively technique for modelling the infilled frame, in current practice, the structure is normally designed as a pure frame and masonry is considered as static load. Researches show that an infilled frame structure without opening actually performs better than a bare frame one against statistic or dynamic forces but when masonry infills have opening, however, the analytical model is again difficult. In this study, masonry infills are considered a building envelope with load-bearing function. A finite element procedure for the effective properties of microcracked viscoelastic masonry based on homogenization technique is provided to take into account the influence of crack density and time. It is also recommended as a simple means of modeling the behavior of the masonry infilled frame with and without opening. The results showed that under statistic loads, the masonry infills even in case with opening much reduce the displacement of frame compared with bare frame and the masonry significantly influences the principal stress field upheaval in the frame. This suggests that it is necessary to take into account the behavior of micro-cracked viscoelastic masonry to evaluate more accurately the global response of frames and the masonry infills with and without opening.

Keywords: *Masonry infills; homogenization; numerical method; micro-cracked viscoelastic masonry; masonry infilled frame.*

1. Introduction

In recent year, infill walls are well known as a load-bearing structure which contributes significantly to the stiffness and resistance of the building. The experimental and analytical results indicate that infill masonry without opening can remarkably improve the performance of reinforced concrete (RC) or steel and that the probability of failure of the frames with regularly distributed infill is much smaller than that of the bare frame [1]. To simulate the contribution of the infills to the overall response of the structure, there are typically three approaches, namely Macro-modelling, Micro-modelling and Micro-macro modelling.

The first one is macro structure model with benefits of computation simplicity and efficiency. A linear equivalent compressive strut model is proposed for computing

* Email: nguyennga@lqdtu.edu.vn

https://doi.org/10.56651/lqdtu.jst.v5.n01.371.sce

maximum strength and stiffness of masonry walls. This strut is made of same material and having the same thickness as the infill panel. The width of strut is equal to one third of the infill diagonal length or investigated by a series of tests [2]. After that, the single strut model has been modified to describe more accurately the local effects resulting from the interaction between the infill panel and the surrounding frame. Several researches have proposed modified diagonal strut model by increasing the number of the points connecting the infill panel to the columns or by changing the location at which the infill transfers load to the columns. However, the complexity and computational effort of these models increase and their properties can be difficult to validate based on experiments. Furthermore, for the case of wall with opening, there is no logic in providing a single diagonal strut connecting the node of frame as done for the cases of fully infilled walls.

The second approach (micro structure models) uses a finite element analysis. It requires modeling of the frame elements, the masonry bricks, as well as interface between the bricks and at the joint between the wall and the frame. It is obvious that when micro-models are used, much more refined analyses on numerous elements are needed compared with macro-models. The computational difficulty of micro structure models requires for a more simplified modeling approach, so a simplified micro-model approach was proposed as can be seen in [3]. However, it still requires a high computational effort.

Meanwhile, the third approach (micro-macro approach) defines for brickwork a Representative Elementary Volume (REV) modeled according to the microscopic approach and then the macro behavior of masonry is identified through various loads applied to the REV. The frame elements are modeled normally like the second approach. For the brickwork, some analytical solutions based on analytical homogenization procedures or equivalent periodic eigenstrain method were applied in [4, 5]. This approach provides a good understanding at local and global scales with a low computational cost even in the non-linear case and in multi-story building design. Besides, it is also a good choice for modeling masonry infilled frame with opening. Although there are many analytical and numerical studies on micro-macro modeling of masonry wall, however, few researches have been considered it as infill masonry wall in contact with frame, especially in case of wall with opening. Therefore, the improvement of numeric modeling techniques is required to capture the physical behavior of the relationship between the infill and frame.

In addition, the non-linear phenomena occurred in masonry infill and in the masonry-frame interface must be adequately considered in the design of masonry infilled frame for the model to be realistic. Creep strains should be accounted for

because it significantly contributes towards the material properties of masonry. Many experimental investigations on the behavior of brittle materials subjected to sustained stresses have been carried out. Similarly to concrete and other materials, at constant stress, masonry can be assumed to be viscoelastic [6, 7]. Besides, the nonlinear mechanical behavior for the masonry is due to the creep behavior of the mortar. Among a number of rheological models examined to predict the creep of mortar, the Modified Maxwell model is likely the most accurate and will be used in this article to describe the mortar joint's creep.

Another problem that may arise in masonry is the decay in material properties associated to cracking. When micro-cracks appear, it may damage masonry elements locally and lose the load bearing capacity of masonry structure which can be accompanied by a facilitation of main structure collapse in dynamic loads (earthquake, blasting load, for example). This is especially important for high buildings, which consist of frame structure and masonry infill.

The goal of this article is to provide finite element procedure for the effective properties of microcracked viscoelastic masonry and to investigate the behavior of infilled frame structure with and without opening.

In Section 2, the basis of periodic approach for effective viscoelastic properties of fractured masonry is reported. In Section 3, the finite element procedure will be describe how to determine the effective behavior of fractured viscoelastic masonry. The behavior of the masonry infilled frame will be considered in Section 4. At last, the role of infill walls will be discussed in Section 5.

2. Periodic approach for effective viscoelastic properties of fractured masonry

We know that the mechanical properties of masonry depend on the mechanical properties of components and their distribution. To realize numerical simulation of viscoelastic masonry, it is necessary to model their behavior. In this study, a hypothesis of safe elastic bricks and micro-cracked linear viscoelastic mortar is supposed. It should be noted that many models seem to be acceptable, among them, the Modified Maxwell (MM) one (see Fig. 1) is chosen because it might be properly able to represent the creep behavior of masonry ages at loading (see [8]). Following this numerical approach, a macro-modelling approach associated with a larger number of degrees of freedom was presented by [9] where rigorous non-linear behavior of the structural elements may be included. Following the micro-macro approach, Anthoine A. was the first person to suggest the use of finite element method (FEM) applied on a REV but his work was limited in the elastic behavior of two components [10]. It is interesting to use this idea to focus on the micro-macro approach where an extension of FEM for the viscoelastic

case will be developed. However, this numeric model cannot be applied directly to a masonry in which one of components (i.e., mortar) is micro-cracked linear viscoelastic. The Laplace-Carson transform is one way to go from the real-time space to symbolic one where the behavior non-aging linear viscoelastic (NALV) of the component becomes linear elastic [11] proposed to identify the best approximate effective behavior of a NALV cracked concrete within the class of Burger models by using the coupling between classical homogenization and Griffith's theory. The idea consists that in the symbolic space, the displacement jump is linearly dependent on the macroscopic stress (dilute scheme) and that the behavior of micro-cracked viscoelastic concrete still follows the same class of model (i.e., Burgers) in the short and long terms. The originality of this work is that we can use this idea to define an effective linear viscoelastic behavior of micro-cracked mortar with Modified Maxwell (MM) model (see Fig. 1) which then has to be used in the periodic homogenization of the heterogeneous masonry.

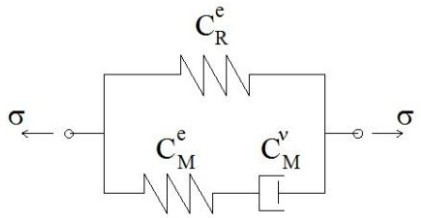

Figure 1. Rheological model for mortar.

2.1. Basic of the periodic approach

In most cases of building practice, brick and mortar are periodically arranged. A micro-macro approach of homogenization based on three steps was proposed. The first step is to define a REV. Reminded that the choice of REV is not unique, as shown in [4, 10]. A good choice can reduce the computational cost. As the considered basic cell plane is symmetrical to two axes, the study carried out on a quarter cell with ordinary boundary conditions resulting from the combination of periodicity and symmetry (see Fig. 2).

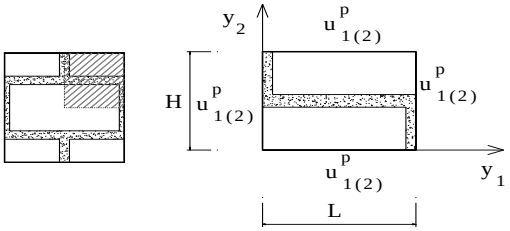

Figure 2. A quarter cell.

Then, the second step consists in analyzing the local consequence of a global load in terms of fields of stress (and strain) in the REV. By applying a uniform displacement load at the edge of VER (see Fig. 3) [10] noted that the macroscopic stress is an average of the stress field in REV as: $\Sigma = \bar{\sigma} = \frac{1}{|S|}\int_S \sigma ds$ with $|S|$ is the total area of *S*. The macroscopic stress can be rewritten by: $\Sigma = \varphi^m \bar{\sigma}^m + \varphi^b \bar{\sigma}^b$ where φ^m and φ^b are respectively volume fractions of mortar and bricks; $\bar{\sigma}^m$, $\bar{\sigma}^b$ are the averages of the stress in mortar and bricks.

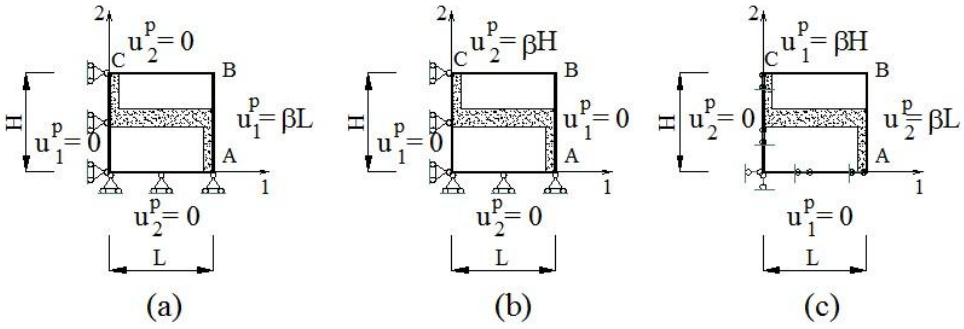

Figure 3. Periodic boundary conditions at the edges of a quarter cell.
Simple displacement u along the first axis (a), the second axis (b) and simple shear (c).

The last step is homogenization, which aims at expression of the behavior of equivalent homogeneous medium. Under the plane stress assumption, the macroscopic tensor of elastic stiffness $\tilde{\mathbb{C}}$ has five independent coefficients to be determined (for more detail, see [10, 12]). Then, equivalent elastic moduli $\tilde{E}_{ij}$ and Poisson's ratios $\tilde{\nu}_{ij}$ are derived by:

$$\tilde{\mathbb{C}} = \begin{pmatrix} \tilde{C}_{1111} & \tilde{C}_{1122} & 0 \\ \tilde{C}_{2211} & \tilde{C}_{2222} & 0 \\ 0 & 0 & \tilde{C}_{1212} \end{pmatrix} = \frac{1}{1-\tilde{\nu}_{12}\tilde{\nu}_{21}} \begin{pmatrix} \tilde{E}_{11} & \tilde{\nu}_{21}\tilde{E}_{11} & 0 \\ \tilde{\nu}_{12}\tilde{E}_{22} & \tilde{E}_{22} & 0 \\ 0 & 0 & \tilde{\mu}_{12}\left(1-\tilde{\nu}_{12}\tilde{\nu}_{21}\right) \end{pmatrix} \quad (1)$$

2.2. Rheological modified maxwell model for viscoelastic mortar

We now discuss the creep behavior of mortar modeled by using a rheological Modified Maxwell model (MM model). In this article, as a class of 3D isotropic NALV, the elastic and viscous stiffness are defined by the following fourth-order tensors:

$$\mathbb{C}_M^e = 3k_M^e\,\mathbb{J} + 2\,\mu_M^e\,\mathbb{K},\ \mathbb{C}_M^v = \eta_M^s\,\mathbb{J} + \eta_M^d\,\mathbb{K},\ \mathbb{C}_R^e = 3k_R^e\,\mathbb{J} + 2\,\mu_R^e\,\mathbb{K},\ \mathbb{C}_R^v = \eta_R^s\,\mathbb{J} + \eta_R^d\,\mathbb{K}$$

with k_M^e, μ_M^e are bulk and shear moduli of the Maxwell series of the mortar without cracks; k_R^e, μ_R^e are bulk and shear moduli of the spring of the mortar without cracks; η_M^s, η_M^d are bulk and shear viscosities of the mortar without cracks.

The elastic and viscous compliance tensors S_M^e, S_M^v is related to the Maxwell part by: $\mathbb{S}_M^e = \frac{1}{3k_M^e}\mathbb{J} + \frac{1}{2\,\mu_M^e}\mathbb{K}$, $\mathbb{S}_M^v = \frac{1}{\eta_M^s}\mathbb{J} + \frac{1}{\eta_M^d}\,\mathbb{K}$. The behavioral law of this model reads:

$$\mathbb{S}_M^v\,\sigma + \mathbb{S}_M^e\,\dot{\sigma} = \mathbb{S}_M^v\,\mathbb{C}_R^e\,\varepsilon + \left(\mathbb{I} + \mathbb{S}_M^e\,\mathbb{C}_R^e\right)\dot{\varepsilon} \tag{2}$$

In the symbolic space of LC, (6) is linear and given by:

$$\mathbb{S}_M^v\,\sigma^* + p\,\mathbb{S}_M^e\,\sigma^* = \mathbb{S}_M^v\,\mathbb{C}_R^e\,\varepsilon^* + p\left(\mathbb{I} + \mathbb{S}_M^e\,\mathbb{C}_R^e\right)\varepsilon^* \tag{3}$$

Since the apparent "stress-strain" relation (3) can be written as $\sigma^* = \mathbb{C}^*\varepsilon^*$ with $\mathbb{C}^* = 3k_s^*\mathbb{J} + 2\,\mu_s^*\mathbb{K}$, so the apparent bulk and shear moduli for the safe mortar can be written as follows:

$$k_s^* = \frac{1}{\dfrac{1}{k_M^e} + \dfrac{1}{p_M^s/3}} + k_R^e, \qquad \mu_s^* = \frac{1}{\dfrac{1}{\mu_M^e} + \dfrac{1}{p_M^d/2}} + \mu_R^e \tag{4}$$

If the derived function of time $\dot{a}$ is $\dot{a} \cong \frac{a(t+dt) - a(t)}{dt}$, the behavior of MM mortar (2) is written:

$$\left(c_5\mathbb{J} + c_6\mathbb{K}\right)\sigma(t+dt) - \left(c_7\mathbb{J} + c_8\mathbb{K}\right)\sigma(t) = \left(c_1\mathbb{J} + c_2\mathbb{K}\right)\varepsilon(t+dt) - \left(c_3\mathbb{J} + c_4\mathbb{K}\right)\varepsilon(t) \tag{5}$$

with

$$c_1 = \frac{3k_R^e}{\eta_M^s} + \frac{1}{dt}\left(1 + \frac{k_R^e}{k_M^e}\right),\ c_2 = \frac{2\,\mu_R^e}{\eta_M^d} + \frac{1}{dt}\left(1 + \frac{\mu_R^e}{\mu_M^e}\right),\ c_3 = \frac{1}{dt}\left(1 + \frac{k_R^e}{k_M^e}\right),\ c_4 = \frac{1}{dt}\left(1 + \frac{\mu_R^e}{\mu_M^e}\right),$$

$$c_5 = \frac{1}{\eta_M^s} + \frac{1}{dt}\frac{1}{3k_M^e},\ c_6 = \frac{1}{\eta_M^d} + \frac{1}{dt}\frac{1}{2\,\mu_M^e},\ c_7 = \frac{1}{dt}\frac{1}{3k_M^e},\ c_8 = \frac{1}{dt}\frac{1}{2\,\mu_M^e}.$$

2.3. Effective behavior of microcracked mortar

The effective behavior of micro-cracked linear viscoelastic concrete was derived from a combination of the Eshelby-based homogenization scheme and the Griffith's theory [11]. In the symbolic space, the apparent effective bulk and shear moduli are respectively given by:

$$\frac{1}{\tilde{k}_{d_c}^*} = \frac{1 + d_c Q^*}{k_s^*},\ \frac{1}{\tilde{\mu}_{d_c}^*} = \frac{1 + d_c M^*}{\mu_s^*} \text{ with } Q^* = \frac{16}{9}\frac{1 - v_s^{*2}}{1 - 2v_s^*},\ M^* = \frac{32}{45}\frac{\left(1 - v_s^*\right)\left(5 - v_s^*\right)}{2 - v_s^*} \tag{6}$$

where k_S^*, μ_S^*, v_S^* are respectively the apparent bulk, shear moduli and Poisson's ratio of the safe mortar. d_c is crack density parameter, $d_c = Nl^3$, N is number of cracks per unit of volume and l is radius of the cracks.

Then, the inversion of the LC transform (ILC) is required to determine the effective behavior in the temporal real space. The presence of cracks makes the formula of moduli complex, so the ILC is carry out exactly only in some simple cases by calculating the integral of Bromwich [13]. It is interesting to approach in the symbolic space the symbolic effective moduli by the ones of an existing rheological model, at least in short and long terms. Nguyen S.T. et al. suggested to use the same model of the safe concrete for the cracked one [11]. In this study, the similar idea is followed to the mortar. We will try to approach the cracked mortar by the MM model (for more detail, see [14]). Therefore, Eqs. (6) can be rewritten by the following conditions:

$$\begin{aligned}
\tilde{k}_{MM}^*\left(p,d_c\right) &= k_R^e\left(d_c\right) + \left[\frac{1}{k_M^e\left(d_c\right)} + \frac{1}{p\eta_M^s\left(d_c\right)/3}\right]^{-1} \\
\tilde{\mu}_{MM}^*\left(p,d_c\right) &= \mu_R^e\left(d_c\right) + \left[\frac{1}{\mu_M^e\left(d_c\right)} + \frac{1}{p\eta_M^d\left(d_c\right)/2}\right]^{-1}
\end{aligned} \tag{7}$$

Using the theorems on the initial and final values: $\lim_{p\to 0} f^*\left(p\right) = \lim_{t\to\infty} f\left(t\right)$; $\lim_{p\to\infty} f^*\left(p\right) = \lim_{t\to 0} f\left(t\right)$, we have the effective stiffness and viscosity parameter related to the MM model:

$$\begin{aligned}
&\frac{1}{k_R^e\left(\mathrm{d_c}\right)} = \frac{1+Q_M^v\mathrm{d_c}}{k_R^e},\ \frac{1}{k_M^e\left(\mathrm{d_c}\right)} = \frac{1+Q_M^e\mathrm{d_c}}{k_R^e + k_M^e - \dfrac{k_R^e\left(1+Q_M^e\mathrm{d_c}\right)}{1+Q_M^v\mathrm{d_c}}} \\
&\frac{1}{\mu_R^e\left(\mathrm{d_c}\right)} = \frac{1+M_M^v\mathrm{d_c}}{\mu_R^e},\ \frac{1}{\mu_M^e\left(\mathrm{d_c}\right)} = \frac{1+M_M^e\mathrm{d_c}}{\mu_R^e + \mu_M^e - \dfrac{\mu_R^e\left(1+M_M^e\mathrm{d_c}\right)}{1+M_M^v\mathrm{d_c}}} \\
&\frac{1}{\eta_M^s\left(\mathrm{d_c}\right)} = \frac{\left(1+Q_M^v\mathrm{d_c}\right)^2}{\eta_M^s\left(1+Q_M^v\mathrm{d_c}\right) - 3\mathrm{d_c}k_R^eQ_1^0},\ \frac{1}{\eta_M^d\left(\mathrm{d_c}\right)} = \frac{\left(1+M_M^v\mathrm{d_c}\right)^2}{\eta_M^d\left(1+M_M^v\mathrm{d_c}\right) - 2\mathrm{d_c}\mu_R^eM_1^0}
\end{aligned} \tag{8}$$

where Q_α^β and M_α^β are given by:

$$Q_M^e = Q_0^\infty = \frac{4}{3}\frac{\left(k_R^e+k_M^e\right)\left[3\left(k_R^e+k_M^e\right)+4\left(\mu_R^e+\mu_M^e\right)\right]}{\left(\mu_R^e+\mu_M^e\right)\left[3\left(k_R^e+k_M^e\right)+\left(\mu_R^e+\mu_M^e\right)\right]},\ Q_M^v = Q_0^0 = \frac{4}{3}\frac{k_R^e\left(3k_R^e+4\mu_M^e\right)}{\mu_M^e\left(3k_R^e+\mu_M^e\right)}$$

$$Q_1^0 = \frac{2}{9}\frac{\left(9k_R^{e2} + 6k_R^e\mu_R^e + 4\mu_R^{e2}\right)\left(-3k_R^e\eta_M^d + 2\mu_R^e\eta_M^s\right)}{\mu_R^{e2}\left(3k_R^e + \mu_R^e\right)^2}$$

$$M_M^v = M_0^0 = \frac{16}{45}\frac{\left(3k_R^e + 4\mu_R^e\right)\left(9k_R^e + 4\mu_R^e\right)}{9k_R^{e2} + 9k_R^e\mu_R^e + 2\mu_R^{e2}}$$

$$M_M^e = M_0^\infty = \frac{16}{45}\frac{\left[3\left(k_R^e + k_M^e\right) + 4\left(\mu_R^e + \mu_M^e\right)\right]\left[9\left(k_R^e + k_M^e\right) + 4\left(\mu_R^e + \mu_M^e\right)\right]}{\left[3\left(k_R^e + k_M^e\right) + \left(\mu_R^e + \mu_M^e\right)\right]\left[3\left(k_R^e + k_M^e\right) + 2\left(\mu_R^e + \mu_M^e\right)\right]}$$

$$M_1^0 = \frac{8}{45}\frac{\left(63k_R^{e2} + 60k_R^e\mu_R^e + 16\mu_R^{e2}\right)\left(3k_R^e\eta_M^d - 2\mu_R^e\eta_M^s\right)}{\left(9k_R^{e2} + 9k_R^e\mu_R^e + 2\mu_R^{e2}\right)^2}$$

For each value of crack density parameter d_c, Eqs. (8) determine characteristics of cracked mortar. The viscoelastic properties of hybrid mortar with or without cracks are given in Table 1.

Table 1. The effective properties of hybrid mortar

d_c	$k_M^e(d_c)$	$\mu_M^e(d_c)$	$\eta_M^s(d_c)$	$\eta_M^d(d_c)$	$k_R^e(d_c)$	$\mu_R^e(d_c)$
0.0	2404	1655	3.35×10^8	1.54×10^8	1257	866
0.1	1846	1440	2.57×10^8	1.33×10^8	965	754
0.2	1498	1275	2.09×10^8	1.19×10^8	784	667

3. The finite element procedure for effective behavior of a fractured masonry wall

3.1. The icremental procedure

Levin et al. ([15]) presented a theorem that can address the homogenization of linear elastic materials with pre-stress or initial deformation. Follow this theorem, macroscopic stress field at the time $(t+dt)$ is written in the form:

$$\sigma(t+dt) = \mathbb{C}_{MM}^{INC}\varepsilon(t+dt) + \sigma_{MM}^p(t) \tag{9}$$

with $\sigma_{MM}^p(t)$ is the pre-stress, which concern the stress and strain at time *t* and given by:

$$\sigma_{MM}^p(t) = -\left(\frac{c_3}{c_5}\mathbb{J} + \frac{c_4}{c_6}\mathbb{K}\right)\varepsilon(t) + \left(\frac{c_7}{c_5}\mathbb{J} + \frac{c_8}{c_6}\mathbb{K}\right)\sigma(t) \tag{10}$$

The stiffness tensor of viscoelastic mortar: $\mathbb{C}_{MM}^{INC} = \frac{c_1}{c_5}\mathbb{J} + \frac{c_2}{c_6}\mathbb{K}$.

For the incremental algorithm, we effectuate as follows:

At t = 0s, instant response is elastic, only the elastic parts of the spring and Maxwell contribute to the rigidity of the material. The constitutive law is: $\sigma_1 = \mathbb{C}_{MM1}^{INC} \varepsilon_1$ with $C_{MM1}^{INC} = C_{RM}^{e} = C_R^e + C_M^e$.

At $t = dt$, the relation between σ_2 and ε_2 reads: $\sigma_2 = \mathbb{C}_{MM2}^{INC} \varepsilon_2 + \sigma_{MM1}^{p}$ where the pre-stress σ_{MM1}^{p} given by (10) is concern of the stress and train σ_1 and ε_1.

Once we have understood the behavior at $t = (i-1).dt$, we will find easily the behavior at time $t = i.dt$. With dt small enough (i.e., $dt = 10^4 s$), we have a very good validation between the numerical calculation and analytically solution [14].

3.2. The numerical approach for two dimensional REV

The calculations are carried out step by step with the finite element method for the time step $dt = 10^4 s$ which is sufficiently small as shown in step of validation (Section 3.1), using the rheological behavior law of mortar (i.e., Modified Maxwell) through an incremental formulation, as seen in Section 3.1, equation (9) for each step. Noted that the relationship between the pre-stress σ_{MM}^{p} expressed at previous time t in the mortar and the fictive nodal force P is:

$$P = \mathbb{A}^m : \sigma_{MM}^{p} \tag{11}$$

with A^m transformation from stress into forces in the mortar.

Acording to the relationship (11), σ_{MM}^{p} is transformed into fictive nodal force on the mortar. This force is an external force on the mortar in addition to displacement load at the edge of VER. Therefore, the overall behavior of the periodic cell is elastic for each step of the time and written in this form:

$$\bar{\sigma}_{\text{cell}}\left(t+dt, d_c\right) = \tilde{\mathbb{C}}_{cell}\left(t+dt, d_c\right) : \bar{\varepsilon}\left(t+dt, d_c\right) \tag{12}$$

We can see that the relation (12) is function of the crack density and time.

Let us evaluate the following properties of a periodic masonry cell (2D) with micro-cracked viscoelastic mortar $d_c = 0.1$, $e^m = 10$ mm $E^b = 11000(\text{MPa}) \approx 2E^m(t=0)$, $\nu^b = 0.2$, under the assumption of plane stress. $\tilde{\mathbb{C}}_{cell}\left(t+dt, d_c\right)$ can be derived by the micro-macro approach of homogenization (see Section 2.1) and then equivalent elastic moduli $\tilde{E}_{ij}$ and Poisson's ratios $\tilde{\nu}_{ij}$ are derived by Eq. (1).

We see in Tab. 2 that when t exceeds 11 days, effective modules tend to a finite asymptotic limit.

Table 2. The effective properties of REV

Time (days)	$\tilde{E}_1(\text{MPa})$	$\tilde{E}_2(\text{MPa})$	$\tilde{G}_{12}(\text{MPa})$	$\tilde{\nu}_{12}$	$\tilde{\nu}_{21}$
0	9761	9257	3821	0.196	0.186
1	8823	7250	2914	0.191	0.156
7	8312	6066	2405	0.186	0.136
11	8305	6060	2403	0.185	0.135

4. Numerical test for in-plane behavior of masonry infilled frame

We consider a two-dimensional masonry infilled RC frame under vertical and horizontal loads performed by [16].

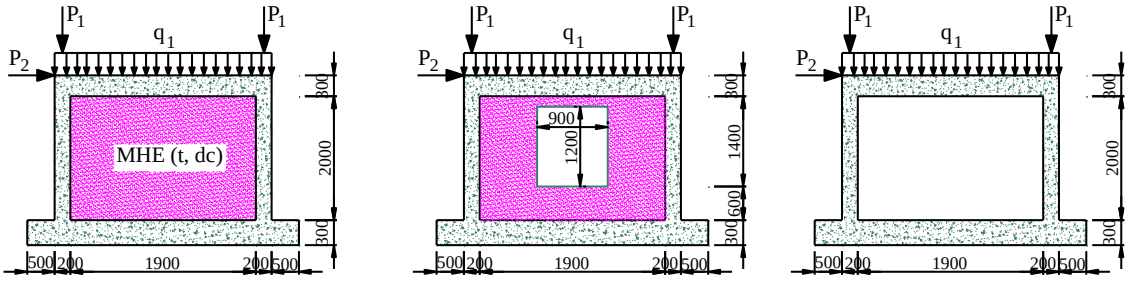

Figure 4. Geometry of three types of frame:
The masonry infilled RC frame without opening (a), with opening (b) and bare frame (c).

As seen in Fig. 4, a constant compressive stress of $q1$ = 0.3 MPa is placed at the top of the frame, represents the gravity load of upper story, a constant concentrated vertical force of P_1 = 100 KN is applied on the top of two columns and a lateral top load P_2 or displacement, in this study, two cases are considered: $P_2 = 50MN$ and $P_2 = 110MN$. Three types of frame are studied: the frame with infilled masonry without opening (a), the frame with infilled masonry with opening (b) and bare frame (c). The opening dimensions are 900 mm (width), 1200 mm (height), represent the width and height of a window. Material properties corresponding to reinforcing concrete assumed for the design are [17]: E_{cr} = 200000 MPa, v_{cr} = 0.2. The effective modules of masonry are given in Table 2 with damage parameter d_c = 0.1 accounting for the time of loading. The masonry is considered as a homogenous material with no distinction between bricks

and mortar. The masonry and the frame are modeled as a series of continuum elements with 1 mm × 1 mm dimensions.

5. Result and discussion

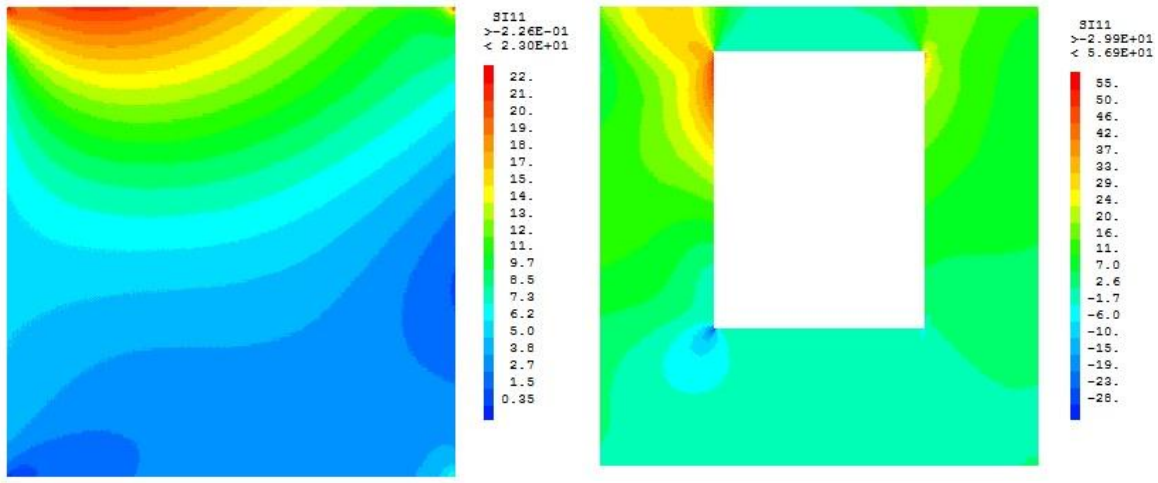

(a) *(b)*

Figure 5. The principle stress in full masonry (a) and in masonry with opening (b).

Figure 5 shows a heterogeneous principle stress local field σ_{11} at t = 11 days, with a compression in the upper horizontal interface near the point of concentrated load P2 and large zones of tension in the right and bottom edges (Fig. 5a). This phenomenon predicts the failure of the wall if the compressive or tensile strengths are exceeded that agrees with experimental collapse in the literature [18]. Besides, in masonry with opening (Fig. 5b), the numerical results for compression zones at the left and right corners of the opening are also in good agreement with the experimental results of [19]. The computational time required for this case was only 16 minutes to simulate 2D micro-cracked viscoelastic masonry infilled frame. Therefore, the coupling between finite element procedure and micro-marco approach offers the possibility of modeling effectively a masonry infilled frame with opening.

In Fig. 6, we can observe that the masonry significantly influences the principle stress field upheaval in the frame in three types of frame. The maximum and minimum of stress are (0.885 MPa; -0.983 MPa), (0.816 MPa; -0.986 MPa), (0.913 MPa; -0.952 MPa) for full masonry, masonry with opening and bare frame, respectively. Fig.6c shows the

stress distribution in the column and concentrated at three points of both left and right columns for the bare frame while the other frames show the stress distribution along both columns and upper beam. Therefore, without masonry wall, the bare frame is more dangerous at internal lateral left top. Figure 7 shows the maximum lateral displacement *Ux* of the modeled frame for three cases of frame. As can be seen, due to the presence of infill masonry (even in case with opening), the displacement is much reduced (52% for full masonry and 38% for opening masonry in average) compared with bare frame.

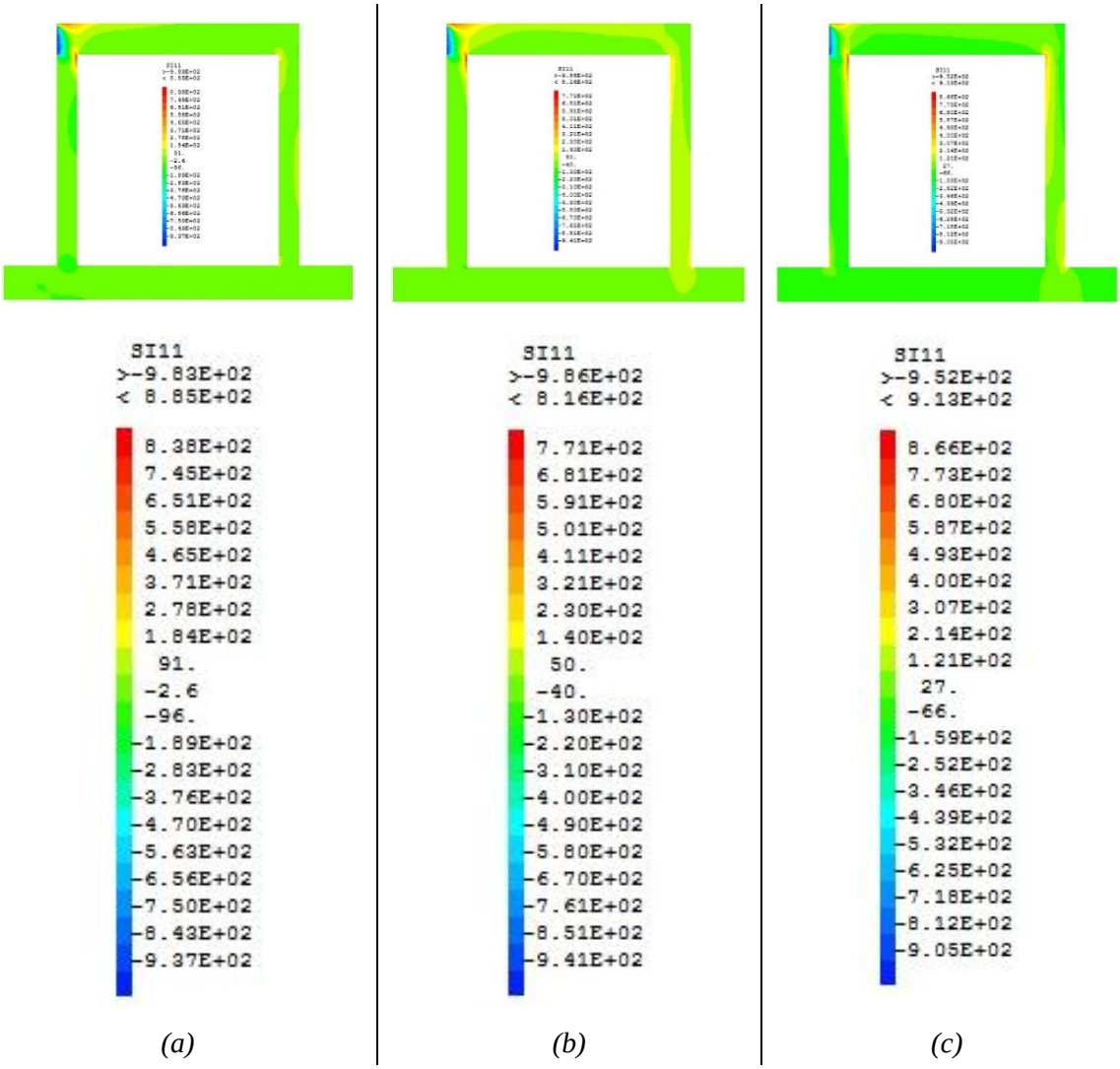

(a) *(b)* *(c)*

Figure 6. The principle stress field upheaval in the frame in case of full masonry (a) masonry with opening (b) and bare frame (c).

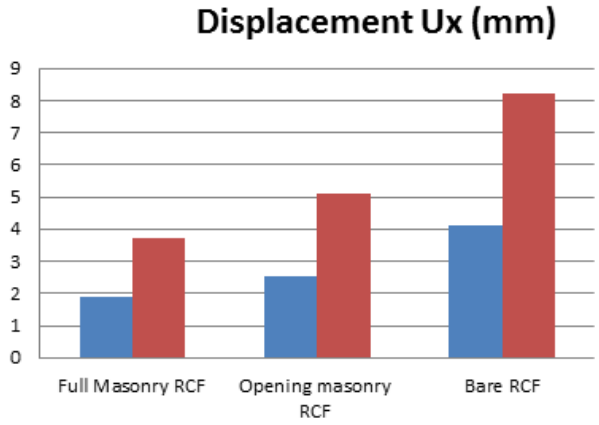

Figure 7. Comparison of maximum displacement in direction x (Ux) among three types of frame for two cases of load P2.

6. Conclusion

In this study, the numerical procedure for effective viscoelastic properties of fractured masonry is outlined based on the periodic multi-scale approach. And then, an application on masonry infilled frame is implemented in open source finite element code to study the effect of micro-cracked viscoelastic masonry infill on the global response of frames.

The results show that the proposed procedure is an effectively technique for modelling masonry infilled frame and the masonry infills with and without opening significantly influence on global response of frames. This suggests that it is necessary to take into account the behavior of micro-cracked viscoelastic masonry to evaluate more accurately the global response of frames. Masonry plays an important role in the global response of frames for both cases with and without opening. Besides, micro-marco approach offers the possibility of modeling effectively a masonry infilled frame with opening compared with micro approach and macro approach.

Future work will devote to study the out-of plane behavior of masonry infilled frames and dynamic loading.

References

[1] Huang, C.H., Tuan Y.A. and Hsu, R.Y., "Nonlinear pushover analysis of frames," *Earthquake Engineering and Engineering Vibration*, Vol. 5, No. 2, Article ID: 1671-3664, 2006, 02-0245-11.

[2] Stafford Smith, B., & Carter, C., "A method of analysis for infilled frames," *Proceedings of the Institution of Civil Engineers*, 44(1), pp. 31-48, 1969.

[3] Abdulla, K. F., Cunningham, L. S., & Gillie, M., "Simulating masonry wall behaviour using a simplified micro-model approach," *Engineering Structures*, 151, pp. 349-365, 2017.

[4] Cecchi, A., & Tralli, A., "A homogenized viscoelastic model for masonry structures," *International Journal of Solids and Structures*, 49(13), pp. 1485-1496, 2012.

[5] Wang, G., Li, S., Nguyen, H. N., & Sitar, N., "Effective elastic stiffness for periodic masonry structures via eigenstrain homogenization," *Journal of Materials in Civil Engineering*, 19(3), pp. 269-277, 2007.

[6] Ignoul, S., Schueremans, L., & Binda, L., "Creep behavior of masonry structures-failure prediction based on a rheological model and laboratory tests," in *Proc. of the 5th int. seminar on structural analysis of historical constructions*, Vol. 2, pp. 913-920, 2006.

[7] Vandoren, B., Heyens, K., & De Proft, K., *Time-dependent mesoscopic modelling of masonry using embedded weak discontinuities*, 2011.

[8] Choi, K. K., Lissel, S. L., & Reda Taha, M. M., "Rheological modelling of masonry creep," *Special Issue on Masonry, Canadian Journal of Civil Engineering*, 34(11), pp. 1506-1517, 2007.

[9] Zucchini, A., & Lourenço, P. B., "A micro-mechanical model for the homogenisation of masonry," *International Journal of Solids and Structures*, 39(12), pp. 3233-3255, 2002.

[10] Anthoine, A., "Derivation of the in-plane elastic characteristics of masonry through homogenization theory," *International Journal of Solids and Structures*, 32(2), pp. 137-163, 1995.

[11] Nguyen, S. T., Dormieux, L., Yann, L. E., & Sanahuja, J., "A Burger model for the effective behavior of a microcracked viscoelastic solid," *International Journal of Damage Mechanics*, 2011, 1056789510395554.

[12] Luciano, R., & Sacco, E., "Variational methods for the homogenization of periodic heterogeneous media," *European Journal of Mechanics-A/Solids*, 17(4), pp. 599-617, 1998.

[13] Beurthey, S., & Zaoui, A., "Structural morphology and relaxation spectra of viscoelastic heterogeneous materials," *European Journal of Mechanics-A/Solids*, 19(1), pp. 1-16, 2000.

[14] Nguyen T.T.N., "Approches multi-échelles pour des maçonneries viscoélastiques," Ph.D. thesis, Université d'Orléans, France, 2015.

[15] Levin, V., Markov, M., & Kanaun, S., "Effective field method for seismic properties of cracked rocks," *Journal of Geophysical Research: Solid Earth*, 1978-2012, 109(B8), 2004.

[16] Lin, K., Totoev, Y. Z., Liu, H., & Guo, T., "In-plane behaviour of a reinforcement concrete frame with a dry stack masonry panel," *Materials*, 9(2), 108, 2016.

[17] Panasyuk, V. V., Marukha, V. I., & Sylovanyuk, V. P., "General characteristics of concretes and reinforced concretes," in *Injection technologies for the repair of damaged concrete structures*, Springer, Dordrecht, 2014, pp. 11-34.

[18] Haris, I., & Hortobágyi, Z., "Comparison of experimental and analytical results on masonry infilled RC frames for cyclic lateral load," *Periodica Polytechnica Civil Engineering*, 59(2), pp. 193-208, 2015.

[19] Bolis, V., & Preti, M., "Openings in infills with horizontal sliding joints: A parametric study to support the design," *Bulletin of Earthquake Engineering*, 17(9), pp. 5101-5132, 2019.

ẢNH HƯỞNG CỦA KHỐI XÂY ĐẾN KHUNG CÓ TƯỜNG CHÈN CÓ VÀ KHÔNG CÓ LỖ MỞ

Nguyễn Thị Thu Nga, Trần Nam Hưng

Tóm tắt: *Ảnh hưởng của khối xây chèn đến sự làm việc tổng thể của khung đã được biết đến rộng rãi nhưng trong mô hình phân tích, điều này thường bỏ qua. Trong thực hành tính toán, vì thiếu kỹ thuật mô phỏng kết cấu khung chèn hiệu quả nên kết cấu thường được thiết kế như khung không khối xây và khối xây thì được coi là tải trọng tĩnh. Các nghiên cứu hiện nay chỉ ra rằng kết cấu khung chèn không có lỗ mở cho ứng xử tốt hơn khung không khối xây khi chịu tải trọng tĩnh hoặc động, tuy nhiên khi khối xây chèn có lỗ mở thì mô hình phân tích gặp khó khăn. Trong nghiên cứu này, khối xây chèn được xem như là kết cấu bao che chịu tải trọng. Thủ tục phần tử hữu hạn cho tính chất hiệu dụng của khối xây đàn nhớt có vết nứt dựa trên kỹ thuật đồng nhất được đề xuất để tính đến ảnh hưởng của mật độ vết nứt và thời gian. Đây cũng là phương tiện khá đơn giản để mô phỏng sự làm việc của khung chèn có và không có lỗ mở. Kết quả cho thấy, dưới tác dụng của tải trọng tĩnh, khối xây chèn ngay cả trường hợp không có lỗ mở đều làm giảm đáng kể chuyển vị của khung so với khung không khối xây và khối xây gây ảnh hưởng đáng kể đến sự biến đổi trường ứng suất chính trong khung. Do đó, cần phải tính đến ứng xử của khối xây đàn nhớt có vi vết nứt để đánh giá chính xác hơn sự làm việc tổng thể của khung và khối xây chèn có và không có lỗ mở.*

Từ khóa: Khối xây chèn; phương pháp đồng nhất; phương pháp số; khối xây đàn nhớt có vết nứt; khung chèn.

Received: 9/4/2022; *Revised:* 4/6/2022; *Accepted for publication:* 20/6/2022

❑